Politecnico di Milano

Prova finale: Introduzione all'analisi di missioni spaziali

AA 2021-2022

Docente:

F. Bernelli Zazzera

Elaborato n. A43

Autori

Cod. Persona	Cognome	Nome
10667313	Castelvetri	Alessandro
10700071	Chiozzi	Alberto
10709049	Curti	Gianni

Data di consegna: 15/11/2021

Table of contents

Glossary

SMA	a	$[km]$	Semimajor axis
ECC	e	$[-]$	Eccentricity
INC	i	$[°]$	Inclination
RAAN	Ω	$[°]$	Right ascension of the ascending node
AOP	ω	$[°]$	Anomaly of pericenter
TA	θ	$[°]$	True anomaly
ALF	α	$[°]$	Spherical angle

1. Introduction

Mathematically speaking, there are virtually infinite possibilities for the transfer from a starting orbit to a destination one in space, as the orbits themselves are paths made of infinite points.
In addition to this, there are five constant parameters plus one variable in the Keplerian system describing an orbit (a, e, i, Ω, ω and θ), and each one can be modified singularly, in couple, in groups of three or four, or all in one single moment.

The choice of the best transfer among all the available courses is the kernel of this paper, driven by the search for a good compromise between the cost, in terms of Δv, and the time required for the maneuver to happen.

The team's modus operandi is heavily based on theory fundamentals, although a lot of effort was put in trying to reach a bias-free starting point after the first transfer, to ensure the best quality of the output, regardless of the habits acquired while studying.

The orbits are calculated and drawn thanks to scripts written by the team, implemented in Matlab® (MathWorks).

2. Initial orbit characterization

2.1. Orbital parameters

The starting orbit, around the Earth, is defined by the following orbital parameters, in parametric and orbital notation:

r_i	$[-5675.1396 \quad -8019.5320 \quad -1740.6945]^T\ km$
v_i	$[3.9050 \quad -2.0080 \quad -4.2550]^T \dfrac{km}{s}$
a_i	$9375.7674\ km$
e_i	$\underline{e}_i = [0.02329 \quad 0.05837 \quad 0.02559]^T \quad e_i = \|\underline{e}_i\| = 0.06786$
i_i	$45.5495°$
Ω_i	$44.7047°$
ω_i	$31.8881°$
θ_i	$162.2579°$

2.2. Interpretation

Given the data above, it is clear that the start orbit is elliptical, being the eccentricity between 0 and 1. Therefore, the period and the specific mechanical energy of the orbit are:

$$T_i = 9034.86\ s \approx 2.5\ h$$
$$E_i = -21.25 \frac{km^2}{s^2}$$

The orbit's apsal points have a radius of $r_{a,i} = 10012.029\ km$ and $r_{p,i} = 8739.505\ km$; given that the apogee and the perigee are below $20000\ km$ and above $5000\ km$, the orbit can be classified as a MEO.
According to the value of the inclination, the orbit is nor equatorial nor polar. Follow a graphic representation of the orbit:

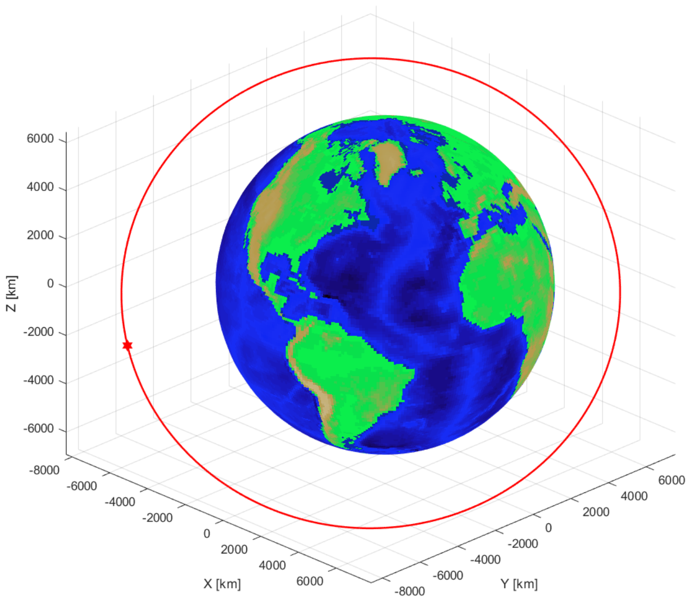

Figure 1: starting orbit

3. Final orbit characterization

The goal orbit, around the Earth as well, is defined by the following orbital parameters, in parametric and orbital notation:

r_f	$[\,13222.8532 \quad 7835.5989 \quad -19715.1085]^T\ km$
v_f	$[-0.6631 \quad 3.2645 \quad -0.0127]^T\ \dfrac{km}{s}$
a_f	$19170\ km$
e_f	$\underline{e}_f = [-0.1324 \quad -0.2350 \quad 0.2403]^T \quad e_f = \lVert\underline{e}_f\rVert = 0.3613$
i_f	$53.6059°$
Ω_f	$101.6427°$
ω_f	$124.2745°$
θ_f	$157.2769°$

3.1. Interpretation

According to the data above, it is clear that the goal orbit is elliptical too, being the eccentricity between 0 and 1. Therefore, the period and the specific mechanical energy of the orbit are:

$$T_f = 26414.60\ s \approx 7.3\ h$$

$$E_f = -10.39\frac{km^2}{s^2}$$

As the start orbit, the specific mechanical energy is negative, but lower in modulus, as the final orbit is further from the attractor. The orbit's apsal points have a radius of $r_{a,f} = 26093.120\ km$ and $r_{p,f} = 12243.879\ km$; consequently, the orbit lays close to the MEO category, but does not belong to it.
The inclinations of the start and goal orbits are separated by a consistent gap, nevertheless the overall properties are maintained: the orbit is nor equatorial nor polar, like the start orbit.

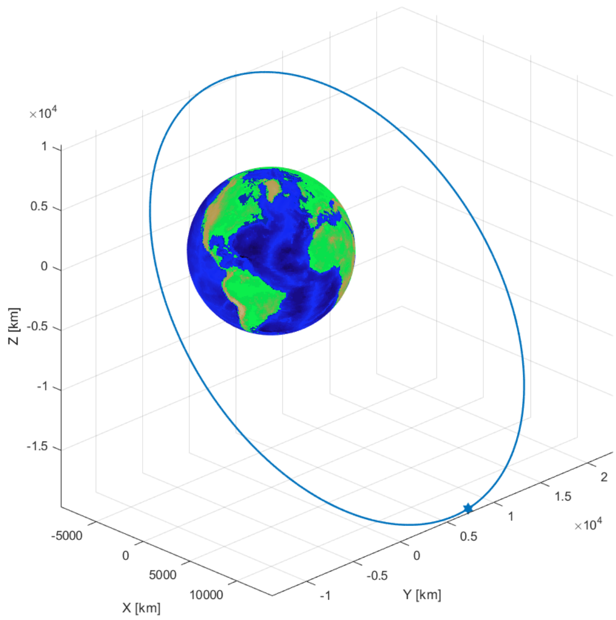

Figure 2: goal orbit

4. Transfer trajectory definition and analysis

The representation of both the orbits in the same picture leads to the conclusion that they share no intersection: the single maneuver option is consequently discarded, as the orbital parameters can be changed in no less than two distinct burns, separated by a certain amount of time.

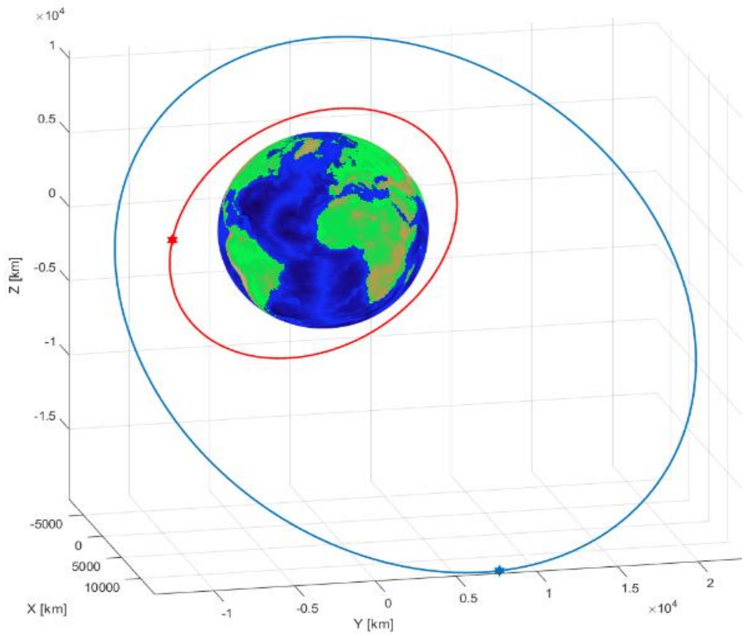

Figure 3: comparison of the two orbits

In the following paragraphs, three different transfers have been designed and considered. The standard strategy reveals the high cost, in terms of Δv, of the plane change maneuver. Furthermore, several options were analyzed in which i_f and Ω_f were reached with different burns, but all the outcomes showed the inefficiency and unsuitability of such transfers. Consequently, two other strategies were designed: they both focus on the minimization of the transversal velocity in the point where the single burn is performed, since α is univocally determined by Δi and $\Delta\Omega$ and it cannot be changed.

4.1. Transfer strategy 1

This strategy allows a fast transfer at the expense of a high Δv_{tot}. The strategy consists of four different burns to reach the target orbit. The first one regards the change of the orbit plane: both Ω and i will have to be changed immediately into the final values, while the spacecraft is in the first orbit near the attractor.

Strategy's milestones:

1. Reaching the position when the change in plane is made ($\Delta t_1 = 6551\ s$)
2. Changing Ω and i with the first burn ($\Delta v_1 = 4.9332\ km/s$)
3. Elapsed time between the point where the plane was changed to the position where ω will be aligned with the final one ($\Delta t_2 = 3688\ s$)
4. 2^{nd} burn to align ω with a difference of phase of $180°$ ($\Delta v_2 = 0.3663\ km/s$)
5. Time to arrive at orbit's pericenter to start the transfer ($\Delta t_3 = 3821\ s$)
6. 3^{rd} burn to start the bitangential transfer to the final orbit ($\Delta v_3 = 0.3185\ km/s$)
7. Time in the transfer orbit ($\Delta t_4 = 5347\ s$)
8. 4^{th} burn to complete the bitangential transfer and arrive at final orbit's pericenter ($\Delta v_4 = 1.4496\ km/s$)
9. Time to reach the assigned true anomaly ($\Delta t_5 = 9988\ s$)

As expected, the orbit plane burn is more expensive close to the attractor than further away. Aligning the AOP with the 2^{nd} burn at a phase displacement of $180°$ allows to save propellant (-9.29%), since the $\Delta\omega$ is reduced and ω_f is reached with the transfer to change a and e. Furthermore, with the phase displacement, the team was able to use a bitangential transfer from the pericenter of the initial orbit to the pericenter of the final one. This maneuver allowed to save about $6091.1\ s$ respect to a case where a transfer pericenter-apocenter was used. Although the Δv for pericenter-pericenter transfer is higher than the pericenter-apocenter option ($+7.5\%$), the chosen architecture is more time-effective (-53.25%).

4.2. Transfer strategy 2

This strategy takes into account the first technique considered to minimize the orbit plane change Δv. Doing the maneuver in a circular orbit is beneficial to the mission, since the eccentricity is nullified: the cost of changing plane is reduced, as well as the cost to align the pericenter's anomaly, that is equal to zero. In fact, the spacecraft simply needs to wait to reach the true anomaly where the last burn is performed to reach the final orbit after changing the plane and AOP.

Strategy's milestones:

1. Time to reach the pericenter from the initial position ($\Delta t_1 = 5025\ s$)
2. 1^{st} burn to start the transfer which will bring the spacecraft at the apocenter of the final orbit ($\Delta v_1 = 1.2893\ km/s$)
3. Time in the transfer orbit ($\Delta t_2 = 11439$ s)
4. 2^{nd} burn to circularize the orbit in the final orbit's apocenter ($\Delta v_2 = 1.1398\ km/s$)
5. Time to reach the position in which the change of plane occurs ($\Delta t_3 = 28886\ s$)
6. 3^{rd} burn to change the orbital plane ($\Delta v_3 = 2.8773\ km/s$)
7. Additional time in the circular orbit to align with ω_f ($\Delta t_4 = 23835\ s$)
8. 4^{th} burn to enter the final orbit in the apocenter ($\Delta v_4 = 0.7848\ km/s$)
9. Time to reach the assigned final point ($\Delta t_5 = 23194\ s$)

The strategy adopted to align the pericenter's anomaly without an additional burn on the final orbit allows to save a considerable amount of propellant, since changing ω in the final orbit would have costed $1.2439\ km/s$ plus the energy required for another transfer to deal with the phase displacement of $180°$.

4.3. Transfer strategy 3

The third transfer is based on a parametrical optimization to find the optimal θ_{burn} for the plane change. The transfer orbit between the initial orbit's pericenter and the final one's apocenter was chosen to perform the maneuver because of its high eccentricity $e_t = 0.4982$. Therefore, a change in plane done in that apocenter's orbit would be more efficient than in the circular trajectory case. However, θ_{burn} depends on ω_i when Δi and $\Delta\Omega$ are fixed, and thus a preliminary change in orbit's AOP can be necessary: this cost must be considered during the trade-off as well.
The team decided to project a "for cycle" in Matlab in which θ_{burn} was the varying parameter, while ω_1 and ω_2 (the AOPs before and after the maneuver) were the outputs.

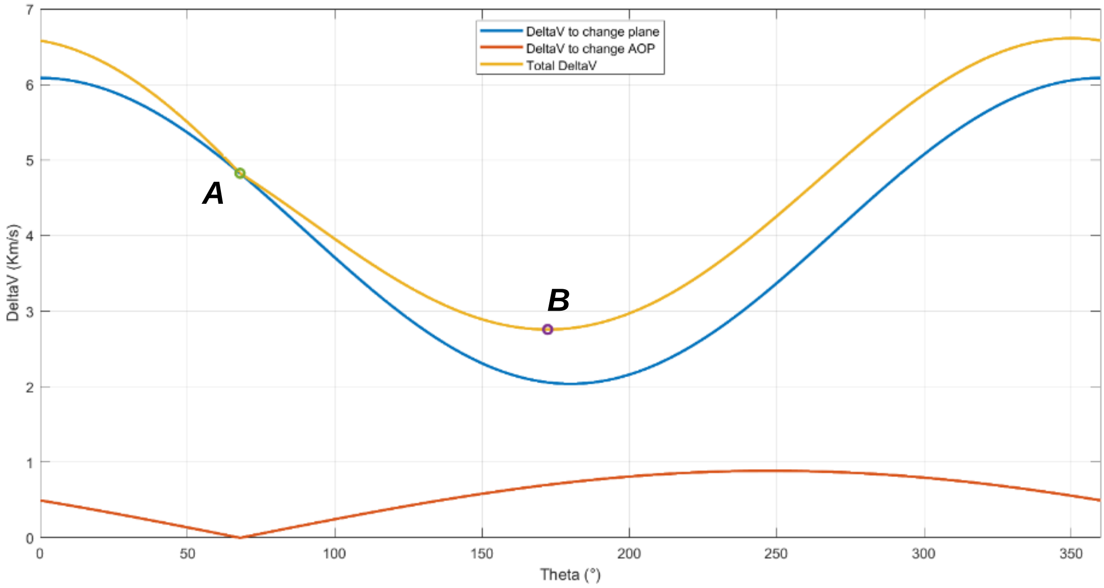

Figure 4: graph showing the partial and total cost of the manoeuvres

The graph was plotted with the data derived from the “for cycle”: point “***A***” represents the cost of the change in the orbital plane if no preliminary change of the AOP is made. It is particularly evident because the corresponding value on the red line, which represents the AOP change cost, is null. Moreover, point “***B***” represents the optimum value ($\theta_{opt} = 172.28°$ with $\omega_1 = 287.48°$) to perform the maneuver. This value is slightly less than $180°$ and this fact allows a time-effective operation, since the change in the plane can be carried out before the apocenter, where the orbit can be immediately circularized to start the alignment with the final pericenter’s anomaly.

Strategy’s milestones:

1. Time to reach the point where the pericenter’s anomaly is changed ($\Delta t_1 = 7753\ s$)
2. 1^{st} burn to change directly ω_i into $\omega_1(\Delta v_1 = 0.7007\ km/s)$
3. Time to reach the first orbit’s pericenter ($\Delta t_2 = 2295\ s$)
4. 2^{nd} burn to enter the transfer orbit ($\Delta v_2 = 1.2893\ km/s$)
5. Time to reach the point of change of plane ($\Delta t_3 = 10177\ s$)
6. 3^{rd} burn to change the plane in θ_{opt} ($\Delta v_3 = 2.0565\ km/s$)
7. Time to reach the apocenter of the transfer orbit ($\Delta t_4 = 1262\ s$)
8. 4^{th} burn to circularize the orbit ($\Delta v_4 = 1.1398\ km/s$)
9. Time in the circular orbit to align with ω_f ($\Delta t_5 = 27460\ s$)
10. 5^{th} burn to enter the final orbit in the apocenter ($\Delta v_5 = 0.7848\ km/s$)
11. Time to reach the assigned final position ($\Delta t_6 = 23195\ s$)

All the graphic representations of the orbits are showed in the “*Conclusions*” section.

5. Conclusions

The proposed orbits both succeed in optimizing the cost of the maneuver to change the orbital plane but at the expense of the total transfer time.

As far as the second strategy is concerned, the Δv_{tot} is substantially reduced (-13.81%) and the cost for changing the orbital plane (-41.67%) too. However, the biggest drawback regards the Δt, since this transfer is almost three times slower than the first one, due to the fact that the chosen radius for the circular orbit is $r_{a,f}$.

The increase in time has been mitigated respect to the second option with a reduction of 19.80% and the Δv has been further optimized as well ($-0.1202\ km/s$). These features make this third option preferrable in each sense to the second one, while an accurate trade-off is needed when it is compared with the first one. The Δv underwent a considerable optimization (-15.51%) at the expense of Δt ($+152.44\%$).

The cost of the orbital plane change has been considerably reduced respect to the second strategy (-28.53%) and the time spent on the circular orbit.

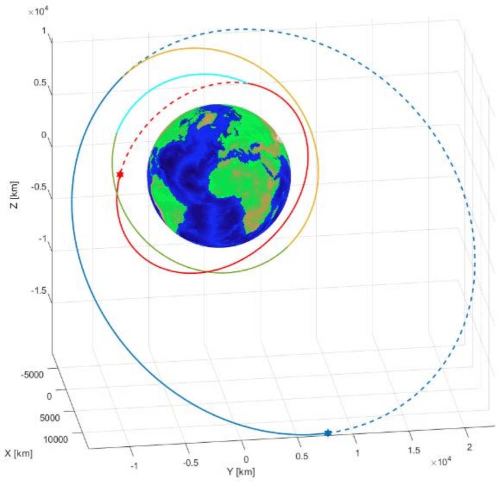

Figure 5: first transfer strategy

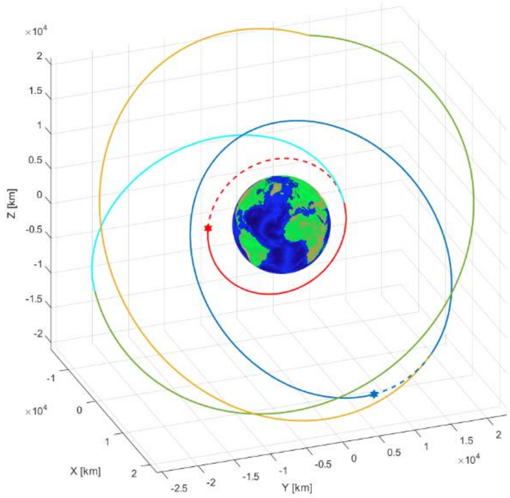

Figure 6: second transfer strategy

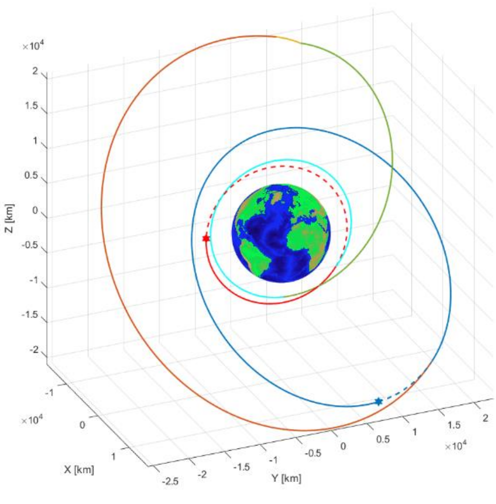

Figure 7: third transfer strategy

Appendix

Table 1: Transfer strategy 1

$t\ (s)$	$a\ (km)$	e	$i\ (°)$	$\Omega\ (°)$	$\omega\ (°)$	$\theta\ (°)$	$\Delta v\ \left(\frac{km}{s}\right)$
0	**9375.73**	**0.0679**	**45.55**	**44.70**	**31.91**	**162.23**	
6551	9375.73	0.0679	45.55	44.70	31.91	67.87	4.9332
	9375.73	0.0679	53.61	101.64	353.06	67.87	
8846	9375.73	0.0679	53.61	101.64	353.06	155.61	0.3663
	9375.73	0.0679	53.61	101.64	304.27	204.39	
12667	9375.73	0.0679	53.61	101.64	304.27	0	0.3185
	10491.70	0.1670	53.61	101.64	304.27	0	
18014	10491.70	0.1670	53.61	101.64	304.27	180	1.4496
	19170	0.3613	53.61	101.64	124.27	0	
28002	**19170**	**0.3613**	**53.61**	**101.64**	**124.27**	**157.28**	**7.0676**

Table 2: Transfer strategy 2

$t\ (s)$	$a\ (km)$	e	$i\ (°)$	$\Omega\ (°)$	$\omega\ (°)$	$\theta\ (°)$	$\Delta v\ \left(\frac{km}{s}\right)$
0	**9375.73**	**0.0679**	**45.55**	**44.70**	**31.91**	**162.23**	
5025	9375.73	0.0679	45.55	44.70	31.91	0	1.2893
	17418	0.4982	45.55	44.70	31.91	0	
16464	17418	0.4982	45.55	44.70	31.91	180	1.1398
	26093.12	0	45.55	44.70	0	211.91	
45350	26093.12	0	45.55	44.70	0	99.76	2.8773
	26093.12	0	53.61	101.64	0	60.93	
52733	26093.12	0	53.61	101.64	0	46.61	0.7848
	19170	0.3613	53.61	101.64	124.27	180	
75928	**19170**	**0.3613**	**53.61**	**101.64**	**124.27**	**157.28**	**6.0913**

Table 3: Transfer strategy 3

$t\ (s)$	$a\ (km)$	e	$i\ (°)$	$\Omega\ (°)$	$\omega\ (°)$	$\theta\ (°)$	$\Delta v\ \left(\frac{km}{s}\right)$
0	**9375.73**	**0.0679**	**45.55**	**44.70**	**31.91**	**162.23**	
7753	9375.73	0.0679	45.55	44.70	31.91	307.79	0.7007
	9375.73	0.0679	45.55	44.70	287.48	52.20	
15627	9375.73	0.0679	45.55	44.70	287.48	0	1.2893
	17418	0.4982	45.55	44.70	287.48	0	
25804	17418	0.4982	45.55	44.70	287.48	172.28	2.0565
	17418	0.4982	53.61	101.64	248.65	172.28	
27066	17418	0.4982	53.61	101.64	248.65	180	1.1398
	26093.12	0	53.61	101.64	0	68.65	
54526	26093.12	0	53.61	101.64	0	304.28	0.7848
	19170	0.3613	53.61	101.64	124.27	180	
77721	**19170**	**0.3613**	**53.61**	**101.64**	**124.27**	**157.28**	**5.9711**